Available online at www.sciencedirect.com
ScienceDirect
Journal of Nuclear Materials 367–370 (2007) 561–567
journal of nuclear materials
www.elsevier.com/locate/jnucmat

On the relation between irradiation induced changes in the master curve reference temperature shift and changes in strain hardened flow stress

G.R. Odette *, M.Y. He, T. Yamamoto

Department of Mechanical Engineering, University of California Santa Barbara, Santa Barbara, CA 93106-5080, United States

Abstract

Irradiation hardening produces increases in the cleavage transition fracture toughness reference temperature (ΔT_0). It is traditional to relate ΔT_0 to the corresponding changes in the yield stress, $\Delta\sigma_y$, as $C_0 = \Delta T_0/\Delta\sigma_y$. However, it is a strain-hardened flow stress, σ_{fl}, in the fracture process zone that controls cleavage, rather than σ_y. Thus irradiation induced decreases in the strain hardening $\Delta\sigma_{sh}$ (<0) must be considered along with $\Delta\sigma_y$ (>0) in evaluating ΔT_0. The $\Delta\sigma_{sh}$ in reactor pressure vessel (RPV) steels irradiated to low doses at around 300 °C are small, even for large $\Delta\sigma_y$. However, the $\Delta\sigma_{sh}$ are much greater for high dose irradiations of tempered martensitic steels (TMS) that are candidates for fusion applications. As a result, for the TMS case, the C_0 are less, and in some instances much less, than for RPV steels and irradiation conditions. We address two key questions. First, how does $\Delta\sigma_{sh}$ influence the $C_0 = \Delta T_0/\Delta\sigma_y$ relation? Second, is it possible to derive a universal relation between ΔT_0 and $\Delta\sigma_{fl}$ averaged over a pertinent range of ε, $\langle\Delta\sigma_{fl}\rangle$, such that a $C_{0'} = \Delta T_0/\langle\Delta\sigma_{fl}\rangle$ is independent of the individual values of $\Delta\sigma_y$ and $\Delta\sigma_{sh}$? The results of this study suggest that $\langle\Delta\sigma_{fl}\rangle$ averaged between 0 and 0.1 provides a similar $C_{0'}$ for various assumptions about the effect of irradiation on $\Delta\sigma_{sh}$. Notably, changes in indentation hardness, ΔH, are also directly related to this same $\langle\Delta\sigma_{fl}\rangle$. Hence, measurements of ΔH should provide a good basis for assessing ΔT_0 for a wide range of alloys and irradiation conditions.

1. Introduction and background

The master curve (MC) method is based on the empirical observation that, in the cleavage transition fracture toughness temperature curves [$K_{Jc}(T)$], for a wide variety of ferritic alloys and alloy conditions, have an approximately constant shape [1–4]. The master curve shape can be indexed on a relative temperature scale [$(T - T_0)$] by a reference temperature (T_0) at 100 MPa$\sqrt{m}$. It is believed that the $K_{Jc}(T - T_0)$ curve is invariant for a wide range of T_0, including following irradiation, leading to T_0 shifts (ΔT_0). It is also well established that shifts in both Charpy indexed (ΔT_c) and fracture toughness (ΔT_0) cleavage transition temperatures induced by neutron irradiation below about 400 °C are primarily due to hardening [1–3,5–7]. Thus it is common to correlate ΔT_c and ΔT_0 with irradiation induced increases in the yield stress ($\Delta\sigma_y$). Analysis

* Corresponding author. Tel.: +1 805 893 3525; fax: +1 805 893 8651.
E-mail address: odette@engineering.ucsb.edu (G.R. Odette).

0022-3115/$ - see front matter © 2007 Published by Elsevier B.V.
doi:10.1016/j.jnucmat.2007.03.045

of data for low dose (typically < 0.06 dpa) ≈ 300 °C irradiations of Mn–Mo–Ni low alloy reactor pressure vessel steels, shows that $C_0 = \Delta T_0/\Delta\sigma_y \approx 0.7 \pm 0.2$ °C [2]. The corresponding values for higher dose (>1 dpa) ≈ 300 °C irradiations of 9Cr tempered martensitic steels (TMS) are generally smaller with $C_0 < \approx 0.6$ °C, and even much less in some cases, particularly for lower irradiation temperatures (T_i) [1,7,12]. Thus it is important to understand and model the mechanisms responsible for differences in C_0. In this paper, we focus on in the hardening dominated embrittlement regime, within the framework of a critical micro-cleavage stress (σ^*)-critical stressed volume (V^*) model of $K_{Jc}(T)$ [1,3,8–11,13,14]. However, in this case we use a two-dimensional small scale yielding model, with T-stresses equal to 0, where the local fracture properties are expressed in terms of a critical area (A^*) within a specified $\sigma_{22} = \sigma^*$ stress contour. Here, σ_{22} is the stress normal to the crack plane. For finite dimensions $V^* = BA^*$, where B is the crack front length, assuming full constraint.

Plausible physical reasons for the lower C_0 observed for the higher dose irradiations of TMS include the following:

- Irradiation induced increases in the critical fracture stress (σ^*) that might be due to decreases in the size of brittle particles that trigger propagating cleavage micro-cracks [1]. However, it is noted that increases in particle size (coarsening), and other irradiation enhanced thermal embrittlement mechanisms, would seem to be more probable, and would presumably lead to decreases in σ^*, hence, larger C_0 [1].
- Decreases in $\Delta\sigma_y$ with increasing test temperature at a specified level of toughness (K_{Jc}) [5,12]. For example, this would contribute to a lower C_0 if room temperature $\Delta\sigma_y$ were used in the assessment when the shifted T_0 is higher. However, the opposite effect might be observed for T_0 less than room temperature.
- Constraint loss in the small fracture specimens that are typically used in irradiation studies of TMS embrittlement [8,10,11,13–15]. Constraint loss is further enhanced by the significant reductions in strain hardening that occurs for the higher dose irradiation conditions [16–18]. The consequence of constraint loss is that the shape of the measured $K_{Jm}(T)$ curve is changed, producing a steeper slope above the lower transition. As a result, the measured irradiated T_0 and ΔT_0 appear to be smaller than that would be observed at full constraint. Note full constraint data generally do not exist for TMS alloys and irradiation conditions. In contrast, since the doses and heating rates are generally much lower than for the TMS case, substantial high constraint data from larger specimens is available for RPV steel irradiations.

While some or all of these factors may be involved in the observed differences in the C_0 between high dose TMS versus low dose RPV steels, we focus here on the direct effects of reductions in strain hardening ($\Delta\sigma_{sh} < 0$) that accompany the increases in $\Delta\sigma_y$ due to irradiation. In assessing the effects of $\Delta\sigma_{sh}$ on ΔT_0 we must consider the effects of irradiation on the *true stress–true strain constitutive law*, not the engineering stress strain curve. In the case of low dose RPV steels, the $\Delta\sigma_{sh}$ are very modest, while they are much larger following high dose TMS irradiations that may even lead to true stress–true strain softening in some cases.

The reason that the effects of $\Delta\sigma_{sh}$ must be considered is that for a specified σ^*, K_{Jc} is controlled by the value of a strain hardened flow stress $[\sigma_{fl}(\varepsilon) = \sigma_y + \sigma_{sh}(\varepsilon)]$ in the process zone region of highly elevated internal stress normal to the crack plane (σ_{22}) in front of a blunting crack tip, rather than σ_y [1,8,13–15]. The true (effective) plastic strains (ε) reach very high values near at the crack tip itself, but drop off rapidly, roughly in proportion to $\approx 1/r$. Cleavage fracture initiates at high stresses with $\sigma_{22}/\sigma_y > 3$ located near, or slightly beyond, the peak stress region [13]. The fracture zone moves closer to the crack tip with increasing toughness and T_t associated with lower σ_{fl}. The peak σ_{22} (σ_{22m}) occurs at a distance of $\approx 2\delta$ from the crack tip, where δ is the crack tip opening displacement. The σ_{22m} roughly scales as $3\sigma_{fl}(0.025)$. Fig. 1 shows typical stress and strain contours assuming a Ramberg Osgood (RO) power law plastic strain hardening model, with $\sigma_{fl}(\varepsilon)/\sigma_y = [\varepsilon/\varepsilon_y]^n$ where ε_y is a yield strain and $n = 0.1$ is the strain hardening exponent. The broad region of the cleavage fracture process zone involved is evident.

As an example, the σ_{22m} are $\approx 3\sigma_y$, $3.4\sigma_y$, $3.85\sigma_y$ and $5\sigma_y$ for a RO $n = 0$, 0.05, 0.1 and 0.2, respectively. For $\sigma_y = 500$ MPa and $\Delta\sigma_y = 300$ MPa, if irradiation reduces the corresponding σ_{sh} to 0 (perfectly plastic behavior), the $\sigma_{22m} = 3 \times 800 = 2400$ MPa. This compares to a $\sigma_{22m} = 3.4 \times 800 = 2720$ MPa if the unirradiated strain hardening law

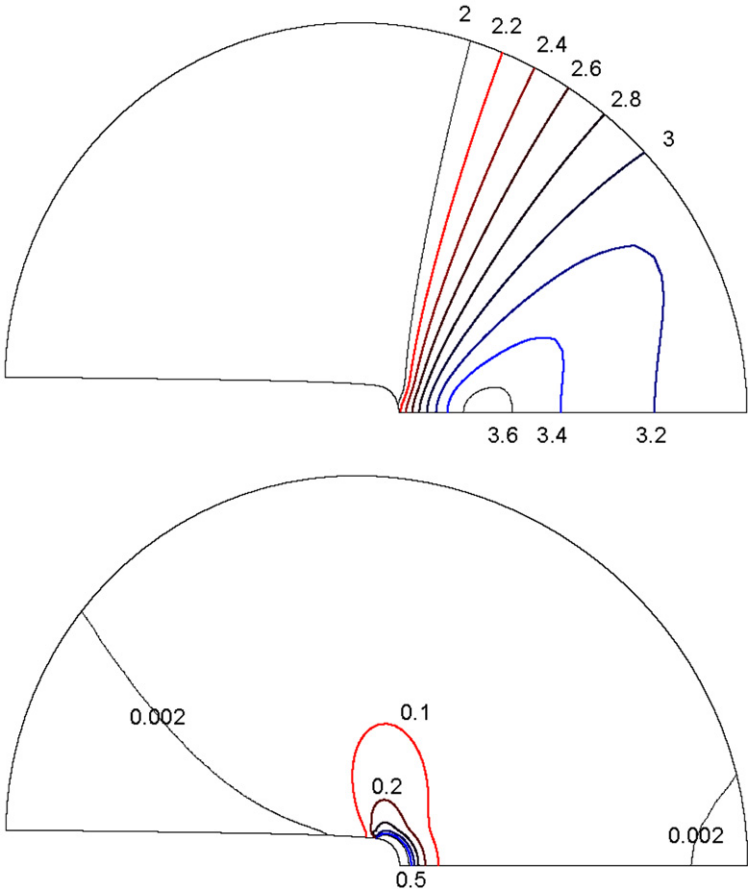

Fig. 1. Typical stress and strain contours for a Ramberg Osgood power law plastic strain hardening model, with $\sigma_{fl}(\varepsilon)/\sigma_y = [\varepsilon/\varepsilon_y]^n$ where ε_y is a yield strain and $n = 0.1$.

persists after irradiation. For the unirradiated condition, the corresponding peak $\sigma_{22} = 3.4 \times 500 = 1700$ MPa. The increase in σ_{22} for the reduced and unaltered strain hardening cases is 700 MPa versus 1020 MPa, respectively. If cleavage was controlled purely by the σ_{22m}, then the $C_0 = \Delta T_0/\Delta\sigma_y$ for the reduced strain hardening case would be about 70% (≈700/1020) of that for the unaltered strain hardening case. However, the actual cleavage process is more complex, and involves the effects of $\Delta\sigma_y$ and $\Delta\sigma_{sh}$ over some range of ε. Thus, we address two key questions. First, how does $\Delta\sigma_{sh}$ influence the $C_0 = \Delta T_0/\Delta\sigma_y$ relation? Second, is it possible to derive a universal relation between ΔT_0 and $\Delta\sigma_{fl}$ at a specified ε, or more likely $\Delta\sigma_{fl}$ averaged over a pertinent range of ε, $\langle\Delta\sigma_{fl}\rangle$, such that $C_0 = \Delta T_0/\langle\Delta\sigma_{fl}\rangle$ is independent of the individual $\Delta\sigma_y$ and $\Delta\sigma_{sh}$. These questions can be addressed within the framework of the σ^*–A^* model.

2. Effects of irradiation on $\sigma_{fl}(\varepsilon)$

Within the framework of the hardening dominated shift model, the $\Delta\sigma_{fl}(\varepsilon)$ is the strength property controlling ΔT_0. Thus it is critical to properly treat the combined effects of irradiation, alloy type, test temperature and strain rate over a proper ε range. Unfortunately, information needed to build appropriate $\sigma_{fl}(\varepsilon)$ models is limited, especially for irradiated alloys with high σ_y and low σ_{sh}, leading to very low to negligible uniform strains, almost immediate necking upon yielding and, in many cases, internal flow localization. Conditions associated with post yield strain softening offer even greater complications. Thus, we will consider general trends between the unirradiated alloys and the corresponding irradiation conditions.

Fig. 2(a) shows an example of the effect of low dose 0.025 dpa, 270 °C irradiation on the room

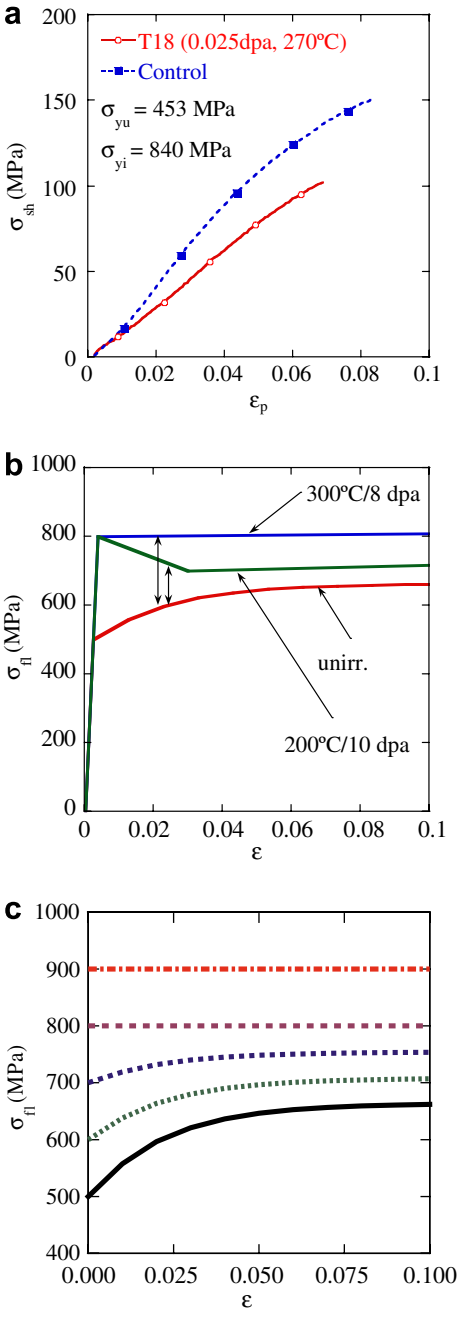

Fig. 2. (a) An example of the effect of low dose 0.025 dpa, 270 °C irradiation on the room temperature $\sigma_{sh}(\varepsilon)$ for high sensitivity (0.2% Cu and 1.6% Ni) RPV steel, (b) $\sigma_{fl}(\varepsilon)$ curves for the F82H TMS unirradiated and irradiated to 10 dpa at 200 °C and 8 dpa at 300 °C, (c) the various $\sigma_{fl}(\varepsilon)$ used for FE simulations.

temperature $\sigma_{sh}(\varepsilon)$ for high sensitivity (0.2% Cu and 1.6% Ni) RPV steel. This data on the CM17 alloy irradiated in the T18 capsule, is part of an enormous database developed by the authors, as part of the US Nuclear Regulatory Commission Irradiation Variables (IVAR) Program. These results will be summarized in future reports and publications; however, specific examples can be obtained upon request of the authors. Note, we show $\sigma_{sh}(\varepsilon)$ rather than $\sigma_{fl}(\varepsilon)$ to make the effects of irradiation on strain hardening more visible. In this extreme case producing a large $\Delta\sigma_y \approx 400$ MPa, $\Delta\sigma_{sh}(\varepsilon)$ is modest; for example, at $\varepsilon = 0.025$, $\Delta\sigma_{sh}(0.025) \approx -20$ MPa. For a lower $\Delta\sigma_y \approx 200$ MPa case (CM19-T16 not shown) the $\Delta\sigma_{sh}(0.025) \approx -10$ MPa. For RPV steels and irradiation conditions, the general trend is $\Delta\sigma_{sh}(0.025) \approx -0.05\Delta\sigma_y$. Thus, irradiation induced $\Delta\sigma_{sh}$ is expected to have little effect on the $C_0 = \Delta T_0/\Delta\sigma_y$ relation for RPV steels. Fig. 2(b) shows the corresponding $\sigma_{fl}(\varepsilon)$ for the TMS F82H. Note the strain hardening in the *unirradiated* TMS alloy is more rapid compared to the RPV steels. For example, at $\varepsilon = 0.025$ the unirradiated σ_{sh} are $\approx$115 MPa and 50 MPa in the unirradiated TMS and RPV alloys, respectively. This difference is the consequence of the finer scale tempered martensite lath packet micro-structure in TMS, compared to the bainitic micro-structure RPV steels [16,19,20].

An even more significant effect is the much larger $\Delta\sigma_{sh}$ following irradiation in the TMS case, leading to approximately perfectly plastic or even softening behavior at high $\Delta\sigma_y$. This is also illustrated in Fig. 2(b) showing two examples of true stress–strain $\sigma_{fl}(\varepsilon)$ curves that were derived using an finite element (FE) procedure, described elsewhere [16]. The procedure is based on simulating engineering stress–strain curves, accounting for geometry and stress state changes that occur during necking, to find a self-consistent $\sigma_{fl}(\varepsilon)$. The $\Delta\sigma_y \approx 300$ MPa for test temperatures (T_t) at T_i in both cases. The curve for a 300 °C, 8 dpa irradiation is almost perfectly plastic, while that for a 200 °C, 10 dpa irradiation shows softening at (≈ -100 MPa at $\varepsilon = 0.025$). Note, the assessment of strain hardening effects is further complicated by the fact that both $\Delta\sigma_y$ (lower) and $\Delta\sigma_{sh}$ (lower or higher) vary with lower $T_t < T_i$, as well as T_i. Nevertheless, as shown by the double arrow lines near $\varepsilon = 0.025$, the $\Delta\sigma_{fl}/\Delta\sigma_y$ are much smaller for TMS alloy and irradiation conditions compared to the RPV steel case. For example, assuming perfectly plastic behavior after irradiation resulting in $\Delta\sigma_y = 300$ MPa, the TMS $\Delta\sigma_{sh}(0.025) \approx -115$ MPa compared to an estimated ≈ -15 MPa for RPV steels and irradiation conditions. Again assuming $\sigma_{fl}(0.025)$ is the controlling strength parameter, the difference in $\Delta\sigma_{sh}(0.025)$

reduces the nominal $C_0 = \Delta T_0/\Delta\sigma_y$ from $\approx$0.7 to $\approx$0.46 °C/MPa. Assuming softening of 100 MPa following irradiation would further reduce C_0 to $\approx$0.3 °C/MPa.

In the section that follows, we further quantify these results based on an σ^*–A^* cleavage model, using prototypical $\sigma_{fl}(\varepsilon)$ that reflect the combined effects of irradiation on both $\Delta\sigma_y$ and $\Delta\sigma_{sh}$, as

$$\sigma_{fl}(\varepsilon) = \sigma_{yu} + \Delta\sigma_y + \sigma_{shu}(\varepsilon) + \Delta\sigma_{sh}(\varepsilon). \quad (1)$$

Here, the subscript u designates the unirradiated condition and the $\Delta\sigma_y$ (>0) and $\Delta\sigma_{sh}(\varepsilon)$ (<0) represent the effects of irradiation on σ_y and σ_{sh}, respectively. Fig. 2(c) shows the various $\sigma_{fl}(\varepsilon)$ we used, based on guidance from assessing trends in a large database. We specifically assume the nominal $\sigma_{shu}(\varepsilon)$ decreases by a factor of 1/3 for $\Delta\sigma_y = 100$ MPa, 2/3 for $\Delta\sigma_y = 200$ MPa and vanishes for $\Delta\sigma_y \geqslant$ 300 MPa.

3. A $K_{Jc}(T)$ master curve model

We have proposed a simple model for small scale yielding that cleavage, by either a single or few propagating micro-cracks, or quasi-cleavage involving extensive micro-cracking prior to cleavage, occurs when a $\sigma_{22} = \sigma^*$ encompass a critical *area* (A^*) [1,7–11,13,14]. Note the actual magnitude of $K_{Jc}(T)$ also depends on the length of the crack front, which is the thickness (B) for a fully constrained though-cracked specimen. We have previously shown that this model is consistent with the master curve $K_0(T - T_0)$ shape at low T_0, assuming that σ^* is approximately independent of temperature. However, at higher temperatures ($T_0 > \approx 0$ °C for low, static strain rates, ε'), a mild temperature dependence of $\sigma^*(T)$ is required to preserve the MC shape due to the corresponding reduction of the temperature dependence of $\sigma_y(T)$ and $\sigma_{fl}(T)$ in the athermal deformation regime. The A^* is assumed to be independent of temperature. The in-plane stressed area $A(\sigma_{22})$ increases with K_J. For SSY conditions $A_{ssy}(\sigma_{22}, K_J)$ increases with K_J^4, and cleavage occurs when $A_{ssy}(\sigma^*, K_{Jc}) = A^*$. The A_{ssy} can be represented in an approximate compact non-dimensional form (A_0) as [8,10,21]:

$$A_0 = -\log[A_{ssy}(\sigma_{22}/\sigma_y)\sigma_y^4/K_J^4]. \quad (2)$$

The $A_0(\sigma_{22}/\sigma_y)$ are computed using finite element (FE) simulations for specified $\sigma(\varepsilon)$, Young's modulus (E) and Poisson's ratio (ν). The numerical results for a given constitutive law can be fitted (C_0, C_1, C_2, ...) to a polynomial as [1,8,21]:

$$A_0(E', \nu, \sigma_{sh}(\varepsilon), \sigma_{22}/\sigma_y) = C_0 + C_1(\sigma_{22}/\sigma_y) + C_2(\sigma_{22}/\sigma_y)^2. \quad (3)$$

Fig. 3(a) shows the $\log A_0$ versus (σ_{22}/σ_y) derived from the FE calculations along with the corresponding polynomial fit lines.

Eqs. (2) and (3) can be used to evaluate K_{Jc} at specified values of $\sigma_{22} = \sigma^*$, $A_{ssy} = A^*$, as

$$K_{Jc}(T) \approx \sigma_y(T)\{A^* 10^{A_0[E,\nu,\sigma_{sh}(\varepsilon),\sigma^*(T)/\sigma_y(T)]}\}^{1/4}. \quad (4)$$

Thus, in the framework of the σ^*–A^* model, the micro-structurally sensitive material properties that control the SSY $K_{Jc}(T)$ are $\sigma_{fl}(\varepsilon, \varepsilon', T)$, A^* and $\sigma^*(T)$, with a much weaker dependence on E and ν. The fit parameters A^* and $\sigma^*(T)$ are the local fracture properties that directly depend, in part,

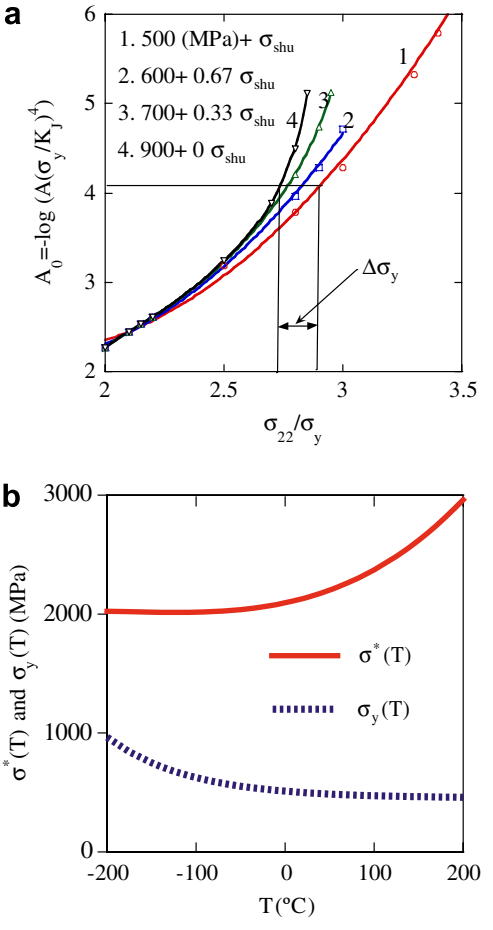

Fig. 3. (a) Log A_0 versus (σ_{22}/σ_y) derived from the FE calculations along with the corresponding polynomial fit lines, and (b) $\sigma^*(T)$ fitted for the $\sigma_y(T)$ derived from the least square fit to RPV and TMS database and $A^* = 5 \times 10^{-9}$ m^2.

on the material micro-structure. The $\sigma^*(T)$ is controlled by the coarse-scale trigger particle microstructure *and* the ferrite lattice toughness controlling the propagation versus arrest of micro-cracks ($K_{\mu a}$) that are nucleated at broken brittle trigger particles. Our hypothesis is that the $K_{\mu a}$ may be a quasi-intrinsic property, weakly dependent on the alloy microstructure, and primarily mediated by the inherent properties of the alloyed bcc ferrite lattice [1,8,22]. The fitting of A^* and $\sigma^*(T)$ is constrained by; (a) the minimum median lower-shelf K_{Jc} of ≈ 30 MPa$\sqrt{m}$, which is sensitive to A^*; (b) the shape of the MC, which is primarily controlled by the temperature dependence of $\sigma_y(T)$ [and $\sigma_{sh}(\varepsilon)$] (known) and $\sigma^*(T)$ (fitted). The reference temperature at 100 MPa$\sqrt{m}$, T_0, or position of the MC on an absolute temperature scale, is primarily controlled by the magnitudes of σ^* and $\sigma_{fl}(\varepsilon)$.

Taking $E = 210$ GPa and $\nu = 0.29$, the fitting resulted in $A^* = 5 \times 10^{-9}$ m^2 and the $\sigma^*(T)$ curve shown in Fig. 3(b). The $\sigma_y(T)$, also shown in Fig. 3(b), was derived from the least square fit to measured yield stress data for a large number of RPV and TMS alloys, adjusted for different σ_y at room temperature. The unirradiated σ_y was taken as 500 MPa in this case.

4. Results and analysis

Fig. 4 shows the $K_{Jc}(T)$ curves for $\Delta\sigma_y$ from 0 to 400 MPa both with (solid lines) and without (dashed lines) corresponding reductions in $\Delta\sigma_{sh}(\varepsilon)$.

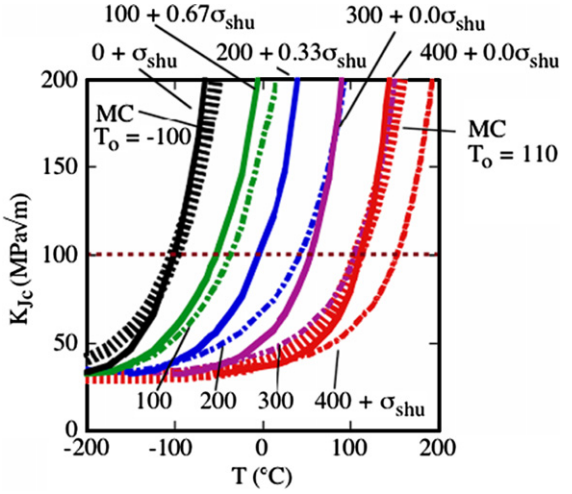

Fig. 4. $K_{Jc}(T)$ curves for $\Delta\sigma_y$ from 0 to 400 MPa both with (solid lines) and without (dashed lines) corresponding reductions in $\Delta\sigma_{sh}(\varepsilon)$.

The predicted $K_{Jc}(T)$ curves (solid lines) are reasonably consistent with the shape MC (wide dashed lines). Fig. 5(a) shows the corresponding ΔT_0 plotted against the $\Delta\sigma_y$. The C_0 found by least square fits are 0.51 °C/MPa for the reduced σ_{sh} case versus 0.66 °C/MPa for the assumption that σ_{sh} is not decreased by irradiation. The nominal relation for RPV steels is also shown for comparison. Fig. 5(a) also shows the effect of strain softening of

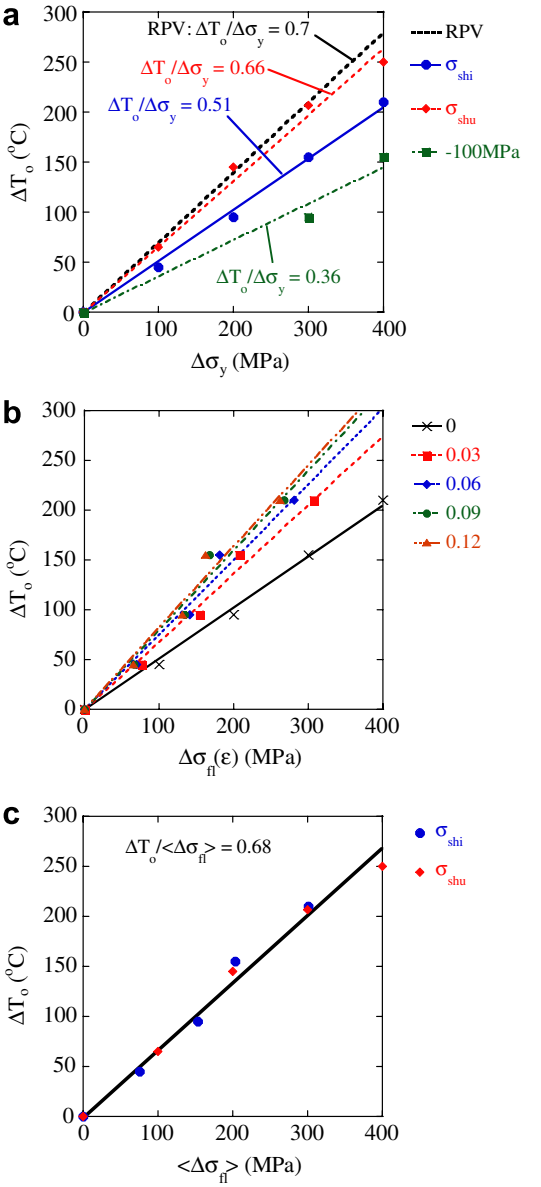

Fig. 5. (a) The corresponding ΔT_0 plotted against the $\Delta\sigma_y$ for various strain hardening cases, (b) $\Delta T_{0'}$ as a function of the $\Delta\sigma_{fl}(\varepsilon)$ for various ε, (c) ΔT_0 versus $\langle\Delta\sigma_{fl}\rangle_H$ for both cases with and without reduction in σ_{sh}.

100 MPa, resulting in a $C_0 \approx 0.36$ °C/MPa for $\Delta\sigma_y = 300$ and 400 MPa resulting in corresponding $\Delta\sigma_{fl} = 200$ and 300 MPa, respectively.

Clearly, irradiation induced decreases in σ_{sh} result in significant reductions in the $C_0 = \Delta T_0/\Delta\sigma_y$ relation. Put simply, part of the $\Delta\sigma_y$ (>0) is wasted (or recovered) by simultaneous $\Delta\sigma_{sh}$ (<0). In principle, this effect could be accounted for by defining ΔT_0 in terms of a $\Delta\sigma_{fl}$ at a specified ε, $C_0 = \Delta T_0/\Delta\sigma_{fl}(\varepsilon)$, or averaged over a pertinent range of ε, $\langle\Delta\sigma_{fl}\rangle$, $C_{0'} = \Delta T_0/\langle\Delta\sigma_{fl}\rangle$. Fig. 5(b) shows $\Delta T_{0'}$ as a function of the $\Delta\sigma_{fl}(\varepsilon)$ for various ε as indicated in the legend. The calculated points approximately fall along the same line with different $C_{0'}$ slopes. The $C_{0'} = 0.69$ °C/MPa at $\varepsilon = 0.03$, which is close to the C_0 for the case where $\Delta\sigma_{fl} = \Delta\sigma_y$, with no reduction in strain hardening. However, it is not clear that a single specified strain is applicable in all cases, and the $C_{0'} = \Delta T_0/\langle\Delta\sigma_{fl}\rangle$ based on averaging $\Delta\sigma_{fl}$ may be more general.

We have shown elsewhere that there is a universal relationship between indentation hardness (H) and the average σ_{fl} between $\varepsilon = 0$ and 0.1, $\langle\sigma_{fl}\rangle_H$ [23,24]. Fig. 5(c) plots ΔT_0 versus $\langle\Delta\sigma_{fl}\rangle_H$ for both cases with and without reduction in σ_{sh}. The ΔT_0 all approximately fall along a single line with $C_{0'} = \Delta T_0/\langle\Delta\sigma_{fl}\rangle_H = 0.68$ °C/MPa. This suggests that there may be a universal relation between ΔT_0 and ΔH (or its $\langle\Delta\sigma_{fl}\rangle_H$ equivalent).

5. Concluding remarks

In this work we addressed two key questions. First, how does $\Delta\sigma_{sh}$ influence the $C_0 = \Delta T_0/\Delta\sigma_y$ relation? Second, is it possible to derive a universal relation between ΔT_0 and $\Delta\sigma_{fl}$ averaged over a pertinent range of ε, $\langle\Delta\sigma_{fl}\rangle$, such that a $C_{0'} = \Delta T_0/\langle\Delta\sigma_{fl}\rangle$ is independent of the individual values of $\Delta\sigma_y$ and $\Delta\sigma_{sh}$. The results suggest that $\langle\Delta\sigma_{fl}\rangle$ averaged between $\varepsilon = 0$ and 0.1 provides a similar $C_{0'}$ for various assumptions about the effect of irradiation on $\Delta\sigma_{sh}$. Notably, changes in indentation hardness, ΔH, are also directly related to this same $\langle\Delta\sigma_{fl}\rangle$. Hence, measurements of ΔH should provide a good basis for assessing ΔT_0 for a wide range of alloys and irradiation conditions.

Acknowledgement

The work was supported by the US Department of Energy, Office of Fusion Science (Grant #DE-FG03-94ER54275).

References

[1] G.R. Odette, T. Yamamoto, H.J. Rathbun, M.Y. He, M.L. Hribernik, J.W. Rensman, J. Nucl. Mater. 323 (2003) 313.
[2] M.A. Sokolov, R.K. Nanstad, ASTM STP 1325 (1999) 167.
[3] G.R. Odette, T. Yamamoto, H. Kishimoto, M. Sokolov, P. Spätig, W.J. Yang, J.-W. Rensman, G.E. Lucas, J. Nucl. Mater. 329–333 (2004) 1243.
[4] ASTM E 1921-05, Standard Test Method for Determination of Reference Temperature, T_0, for Ferritic Steels in the Transition Range, ASTM, 2005.
[5] T. Yamamoto, G.R. Odette, H. Kishimoto, J.-W. Rensman, P. Miao, J. Nucl. Mater. 356 (2006) 27.
[6] R. Kasada, T. Morimura, A. Hasegawa, A. Kimura, J. Nucl. Mater. 299 (2001) 83.
[7] G.R. Odette, H.J. Rathbun, J.W. Rensman, F.P. van den Broek, J. Nucl. Mater. 307–311 (2002) 1624.
[8] G.R. Odette, K. Edsinger, G.E. Lucas, E. Donahue, ASTM STP 1329 (1998) 298.
[9] G.R. Odette, M.Y. He, J. Nucl. Mater. 283–287 (2000) 120.
[10] G.R. Odette, M.Y. He, J. Nucl. Mater. 307–311 (2002) 1624.
[11] H.J. Rathbun, G.R. Odette, M.Y. He, T. Yamamoto, Eng. Fract. Mech. 73 (2006) 2723.
[12] J.-W. Rensman, NRG Irradiation Testing: Report on 300 °C and 60 °C Irradiated RAFM Steels, NRG Petten 20023/05.68497/P.
[13] K. Edsinger, G.R. Odette, G.E. Lucas, B.D. Wirth, ASTM STP 1270 (1996) 670.
[14] G.R. Odette, J. Nucl. Mater. 212–215 (1994) 45.
[15] T.L. Anderson, Fracture Mechanics: Fundamentals and Applications, 3rd ed., CRC Press, Boca Raton, Florida, 2005.
[16] G.R. Odette, M.Y. He, E.G. Donahue, P. Spatig, T. Yamamoto, J. Nucl. Mater. 307–311 (2002) 171.
[17] A.F. Rowcliffe, J.P. Robertson, R.L. Klueh, K. Shiba, D.J. Alexander, M.L. Grossbeck, S. Jitsukawa, J. Nucl. Mater. 258–263 (1998) 1275.
[18] J. Rensman, H.E. Hofmans, E.W. Schuring, J. van Hoepen, J.B.M. Bakker, R. den Boef, F.P. van den Broek, E.D.L. van Essen, J. Nucl. Mater. 307–311 (2002) 250.
[19] P. Spätig, R. Schäublin, M. Victoria, in: H.M. Zbib, G.H. Campbell, M. Victoria, D.A. Hughes, L.E. Levine (Eds.), Material Instabilities and Patterning in Metals, Mater. Res. Soc. Symp. Proc., Spring meeting, vol. 683E, MRS, Warrendale, PA, USA, 2001, BB1.10.1.
[20] P. Spatig, G.R. Odette, G.E. Lucas, M. Victoria, J. Nucl. Mater. 307–311 (2002) 536.
[21] M. Nevalainen, R.H. Dodds, J.R. Rice, J. Mech. Phys. Solids 21 (1973) 131.
[22] M.L. Hribernik, G.R. Odette, M.Y. He, Fusion Materials Semiannual Report 1/1 to 6/30/2005 DOE/ER-313/38 (2005) 109.
[23] G.R. Odette, M.Y. He, D. Klingensmith, Fusion Materials Semiannual Report 7/1 to 12/31/2004 DOE/ER-313/37 (2005) 109.
[24] M.Y. He, G.R. Odette, T. Yamamoto, D. Klingensmith, J. Nucl. Mater., in press, doi:10.1016/j.jnucmat.2007.03.044.